Accepted Manuscript

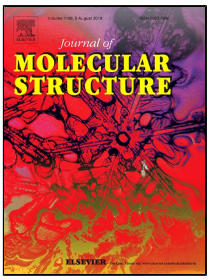

Synthesis, Characterization and DFT studies of a New Unsymmetrical Dinuclear Vanadium(IV) Complex with a bipodal N_2O-donor Ligand

Paula M.A. Machado, Rafael A. Allão Cassaro, Vagner M. de Assis, Sérgio de P. Machado, Adolfo Horn, Elizabeth Roditi Lachter

PII:	S0022-2860(19)30507-1
DOI:	10.1016/j.molstruc.2019.04.098
Reference:	MOLSTR 26470
To appear in:	*Journal of Molecular Structure*
Received Date:	20 December 2018
Accepted Date:	24 April 2019

Please cite this article as: Paula M.A. Machado, Rafael A. Allão Cassaro, Vagner M. de Assis, Sérgio de P. Machado, Adolfo Horn, Elizabeth Roditi Lachter, Synthesis, Characterization and DFT studies of a New Unsymmetrical Dinuclear Vanadium(IV) Complex with a bipodal N_2O-donor Ligand, *Journal of Molecular Structure* (2019), doi: 10.1016/j.molstruc.2019.04.098

Synthesis, Characterization and DFT studies of a New Unsymmetrical Dinuclear Vanadium(IV) Complex with a bipodal N_2O-donor Ligand

Paula M. A. Machado[1], Rafael A. Allão Cassaro[2], Vagner M. de Assis[2], Sérgio de P. Machado[2], Adolfo Horn Jr.[3], Elizabeth Roditi Lachter[1]*.

[1]*Universidade Federal do Rio de Janeiro, Departamento de Química Orgânica, Rio de Janeiro, Brazil*

[2]*Universidade Federal do Rio de Janeiro, Departamento de Química Inorgânica, Rio de Janeiro, Brazil*

[3]*Universidade Estadual do Norte Fluminense Darcy Ribeiro, Laboratório de Ciências Químicas, Campos dos Goytacazes, Brazil*

**lachter@iq.ufrj.br*

Abstract

A new dinuclear vanadium(IV) complex $[(VO)_2(\mu\text{-HBPA})_2(\mu\text{-}SO_4)].4.75H_2O$ was synthesized by the reaction between a bipodal a N_2O-donor ligand N-(2-hydroxybenzyl)-N-(pyridin-2-ylmethyl)amine (HBPA) and vanadyl sulfate. The complex was characterized by elemental analysis, thermogravimetric, electrochemical analysis, ESI-MS, FT-IR and UV-visible. The structure was determined by single crystal X-ray diffraction. The two non-equivalent vanadium(IV) ions are hexacoordinated being bridge-coordinated by the oxygen atoms from of HBPA and sulfate group. The complex was studied by DFT calculations and showed high polarity.

Keywords: Vanadium complex, binuclear, crystal structure, DFT calculation.

Graphical Abstract

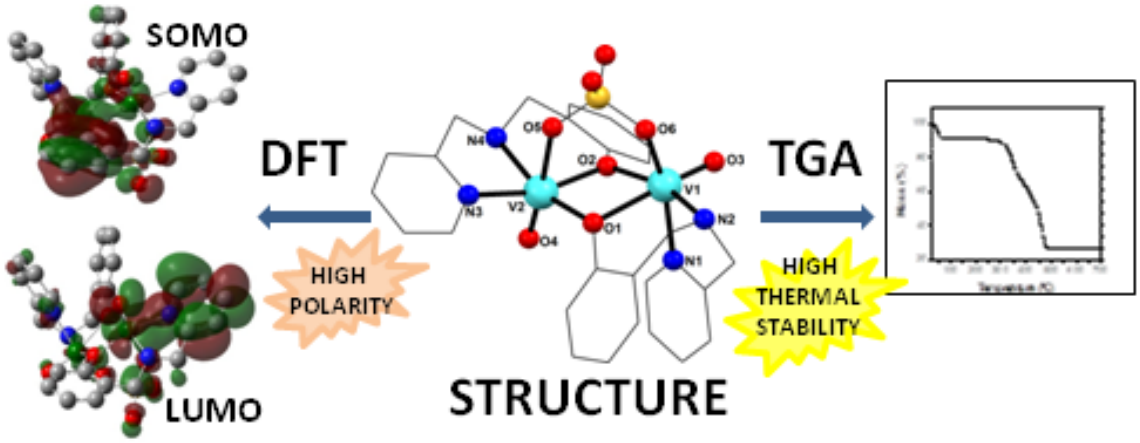

Highligths

- A new binuclear vanadium(IV) complex was synthesized.
- DFT studies show a very high polarity for the complex.
- Thermogravimetric analysis indicates a high thermal stability of the dessolvated complex.

1. Introduction

Vanadium-based compounds have received attention in the last years due to its structural particularities, versatility at applications in biological activities [1] and as catalyst for many processes, mainly oxidation reactions [2, 3, 4]. Vanadium complexes have been extensively applied in medicine studies, as insulin mimetic *in vivo* [5] and *in vitro* tests (1), in the inhibition of cancer cells proliferation [7, 8], as anti-inflammatory, antibiotic [9], antifungal [10], antioxidant agent [11] and emerged as a potential agent for the neglected parasitic diseases such as leishmaniasis and trypanosomiasis [12, 13]. Vanadium has an important role in biological systems, as in some enzymes present in brown seaweed, bacteria, fungi and others organisms [14]. The activity of these enzymes containing vanadium ions in oxidizing halide ions and biosynthesizing brominated compounds has inspired the study of this metal as catalyst in chlorination and bromination reactions [15, 16]. Some vanadium-based coordination compounds catalyzed oxygen transfer reactions [17] to substrates

containing sulfides [18], alkenes [19, 20] as well as epoxidation reactions [21]. Recently, mononuclear and weakly magnetic vanadyl complexes have been considered potential for application as spin qubits for quantum information processing [22, 23, 24].

In view of the great multifunctionality of vanadium complexes, there is a large contribution of the literature in the synthesis, characterization and application of these compounds, mainly about vanadium-based coordination compounds containing N,O donor atoms ligands [25, 26]. Schiff base ligands, containing phenol and imine, as well ligands with amines and pyridines electronic donors produce different structural complexes, as mononuclear vanadium (IV) metal center with penta and six-coordination [25, 26] or binuclear oxovanadium complexes [27, 28]. In particular, ligands containing phenol moieties have been shown ability to form phenoxide bridges leading to multinuclear complexes, including with vanadium ions [28, 29].

In this work, we describe a new dinuclear vanadium(IV) coordination compound containing the ligand N_2O-donor called HBPA (with amine, pyridine and phenol donor groups) and coordinated sulfate. To the best of our knowledge it is the first example of dinuclear vanadium complex containing the metal ions with *fac*- and *mer*-coordination environments. The structure of the complex was determined by single-crystal X-ray. DFT studies shown high polarity and stability for the molecule.

2. Experimental

2.1. Materials

All chemicals and solvents were used without further purifications. The chemicals 2-(aminomethyl)pyridine, salicylaldehyde, vanadyl sulfate, dichloromethane and 2-propanol were purchased from Sigma-Aldrich, USA. Anhydrous magnesium sulfate and sodium borohydride were obtained from VETEC, Brazil, while acetonitrile and dimethylsulfoxide were purchased from ISOFAR, Brazil, and Grupo Química, Brazil, respectively.

2.2. *Characterization*

FTIR analyses were carried out on a Fourier Nicolet Magna-IR 760 using CsI pellets in the range 4000-150 cm^{-1}. Ultraviolet-visible spectra were recorded in the range from 200 to 900 nm, using a Shimadzu UV-1800 spectrometer. Solution ^{1}H NMR was recorded on a Bruker AV500 spectrometer. Elemental analyses (CHN) were carried out on a Perkin Elmer 2400 series II. Thermal analysis was recorded on a TGA-50 Shimadzu, performed under nitrogen flux of 50 mL min^{-1}. The sample was heated from 25 °C to 700 °C using a 2 °C min^{-1} rate and a 10 °C min^{-1} rate from 700 °C to 1000 °C. Cyclic voltametry was performed on a potentiostat PGSTAT100, from Autolab, equipped with a carbon glass as work electrode and Ag/AgCl (saturated) as reference electrode. The complex was analyzed in $1.4x10^{-3}$ mol L^{-1} in methanol solution, using tetrabutylammonium hexafluorophosphate in 0.10 mol L^{-1} as transport electrolyte. Electrospray ionization mass spectra were obtained on a Bruker MicroTOF spectrometer [ESI-(+)-MS], prepared with a collision cell RF in 650.0 Vpp and the capillary in 4500 V with the nebulizer in 0.4 bar, the temperature of dry heater was 180 °C, and the dry gas flow was 4.0 L min^{-1}, employing methanol as solvent.

2.3. *X-ray crystallography*

Single crystal X-ray data were collected on a Bruker D8 Venture diffractometer using graphite monochromatic MoKα radiation (λ = 0.71069 Å) at room temperature. Data collection and cell refinement were performed with Bruker Instrument Service and APEX2 software, respectively. Data reduction was carried out using Bruker SAINT V8.37A software [30]. Empirical multiscan absorption correction using equivalent reflections was performed using the SADABS program [31]. The structure solution was performed using SHELXS-97 while the refinement was performed using SHELXL-2014/7 based on F^2 through the full-matrix least-squares routine [32]. All non-hydrogen atoms were refined

with anisotropic displacement parameters. Hydrogen atoms were located in the difference Fourier map and were also placed in calculated positions and refined isotropically using a riding model [33]. Large thermal displacement parameters were found for lattice water molecules due to disorder. EADP, ISOR and DELU commands were used in the refinement of the disordered solvent. Summary of data collection and structure refinement is shown in Table 1.

Table 1. Summary of data collection and structure refinement.

Identification	$[(VO)_2(\mu\text{-HBPA})_2(\mu\text{-}SO_4)].4.75H_2O$
Formula	$C_{26}H_{37}N_4O_{13.5}SV_2$
Fw (g mol^{-1})	732.45
T (K)	289(2)
λ (Å)	0.71073
Crystal system	Monoclinic
Space group	*C2/c*
a (Å)	26.8357(13)
b (Å)	18.1154(9)
c (Å)	13.6568(6)
α(°)	90
β(°)	98.131(2)
γ(°)	90
Volume (Å^3)	6572.4(5)
Z	8
ρ_{calc} (Mg m^{-3})	1.480
μ (mm^{-1})	0.699
F(000)	2992
θ range(°)	2.25-26.40
Index ranges	-33 ≤ *h* ≤ 33
	-22≤ *k* ≤ 22
	-17≤ *l* ≤ 17
Data collected	52806
Independent reflections	6736

R_{int}	0.0443
Refinement method	Full-matrix least-squares on F^2
Data / restraints / parameters	6736 / 18 / 428
GOF on F^2	1.086
R1, wR2 [I>2σ(I)]	0.0517, 0.1499
R1, wR2 (all)	0.0696, 0.1675
$\Delta\rho_{max}$, $\Delta\rho_{min}$ (e·Å^{-3})	0.885, -0.45

2.4. Density functional theory (DFT) calculations

The DFT calculations were performed using B3LYP level and LANL2DZ basis set in Gaussian 09 software [34]. The ground state geometries were fully optimized considering the complex in the gas phase, starting from the crystal structure omitting the lattice water molecules. Theoretical studies were performed in order to obtain information about hardness, charge distribution and the frontier orbitals, Highest Occupied Molecular Orbital (HOMO) and Lowest Unoccupied Molecular Orbital (LUMO), which are directly related to the reactivity and hardness of the molecule.

2.5. Synthesis of the ligand N-(2-hydroxybenzyl)-N-(pyridin-2-ylmethyl)amine

The ligand HBPA (N-(2-hydroxybenzyl)-N-(pyridin-2-ylmethyl)amine) was synthesized according to a previously described procedure [35]. The ligand was obtained by condensation of 2-(aminomethyl)pyridine (6.3 g, 58 mmol) and salicylaldehyde (7.1 g, 58 mmol) in 50 mL of methanol at room temperature under stirring for 1 hour, followed by subsequent slowly addition of $NaBH_4$ (2.2 g, 58 mmol) in ice bath. Then, the solvent was evaporated and the product was dissolved in 50 mL of dichloromethane, and washed with distilled water. The organic phase was dried with anhydrous $MgSO_4$, which was filtered off. Some hours later, the colorless crystalline product was obtained and washed with cold 2-propanol. M.p.= 62–63°C, yield = 69 %, 8.6 g. ^{1}H NMR (ppm) in $CDCl_3$: 8.57

(dd, 1 H), 7.66 (dt, 1 H), 7.20 (m, 3 H), 7.00 (d, 1 H), 6.89 (d, 1 H), 6.77 (dt, 1 H), 4.02 (s, 2 H), 3.95 (s, 2 H).

2.6. Synthesis of the complex [$(VO)_2$(μ-HBPA)$_2$(μ-SO_4)].4.75H_2O

The complex [$(VO)_2$(μ-HBPA)$_2$(μ-SO_4)].4.75H_2O was obtained by the reaction between HBPA ligand (0.214 g, 1.0 mmol) and $VOSO_4.2H_2O$ (0.163 g; 1.0 mmol) dissolved in 30 mL of 1:1 acetonitrile and methanol solution, under constant stirring for 2 hours at 75 °C, resulting in a dark violet solution. Dark purple single crystals were obtained after keeping the solution at room temperature for 72 hours. Crystal yield = 0,37 g, 49%. Elemental analysis calculated for [$(VO)_2$(μ-HBPA)$_2$(μ-SO_4)].4.75H_2O, C, 42.09, H, 4.82, N, 7.55% found C, 42.99, H, 4.61, N, 7.48%. The crystals can show loss of water molecules after many days at room temperature. ESI-(+)-MS, m/z: 298.1, 608.1, 657.0, 795.5, 871.1, 936.1. Calculated for $C_{26}H_{26}N_4O_8SV_2$, ([$(VO)_2$(μ-HBPA)$_2$(μ-SO_4)]), M^+ 656.5 g found 657.

3. Results and discussion

3.1. Crystal structure

The complex [$(VO)_2$(μ-HBPA)$_2$(μ-SO_4)].4.75H_2O crystallizes in a monoclinic system. The asymmetric unit consists in a dinuclear V(IV) complex, where each metal ion has a N_2O_4 coordination environment and 4.75 lattice water molecules. Each vanadium(IV) ion is in a distorted octahedral geometry being coordinated by one oxygen atom and two nitrogen atoms from phenoxide, amine and pyridine moieties of HBPA ligand, respectively. The other positions are occupied by two oxygen atoms from sulfate and oxo groups. The phenoxide moiety and sulfate groups are bridge-coordinated to the metal ions (Fig. 1). Selected bond lengths and bond angles are gathered on Table 2. Both vanadium(IV) ions are coordinated by the same donor atoms, however the bond lengths, bond angles and distortion on the deprotonated HBPA ligand make the

coordination environment of them quite different. The shortest bond length is vanadium-oxygen atom from oxo group (V1—O3 and V2—O4), while the longest ones are V1—O1 (phenoxide moiety) and V2—O5 (sulfate group). The tridentate deprotonated HBPA coordinated to V2 adopts a meridional conformation while a facial one is adopted when this ligand is coordinated to V1. To the best of our knowledge it is the first example of dinuclear vanadium complex containing the metal ions with *fac*- and *mer*-coordination environments. The intramolecular distance between vanadium(IV) ions is 3.2234(8) Å, while the shortest intermolecular distance between these ions (V1···V1^{i}i =1.5-x; 0.5-y, 1-z) is 6.1096(8) Å.

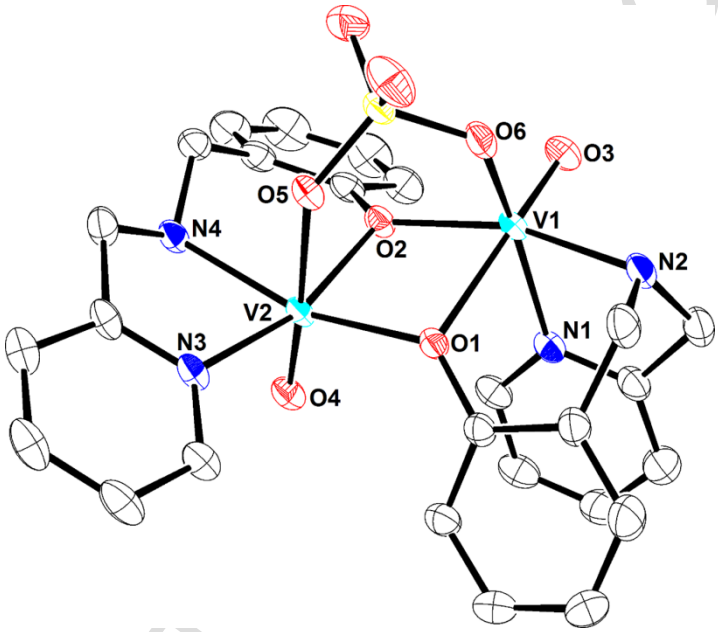

Fig. 1. ORTEP view of the asymmetric unit of $[(VO)_2(\mu\text{-HBPA})_2(\mu\text{-}SO_4)].4.75H_2O$ with thermal ellipsoids at 30% of probability. Hydrogen atoms and oxygen of water molecules were omitted for the sake of clarity. Color code: carbon, nitrogen, oxygen, sulfur atoms and vanadium(IV) ion stands for black, blue, red, yellow and cyan, respectively.

Table 2. Bond lengths and bond angles for $[(VO)_2(\mu\text{-HBPA})_2(\mu\text{-}SO_4)].4.75H_2O$.

Bond lengths (Å)			
V1—O1	2.242(2)	V2—O1	2.017(2)
V1—O2	2.014(2)	V2—O2	2.013(2)
V1—O3	1.592(3)	V2—O4	1.594(2)

V1—O6	1.987(3)	V2—O5	2.193(2)
V1—N1	2.122(3)	V2—N3	2.121(3)
V1—N2	2.116(3)	V2—N4	2.123(3)

Bond angles (°)			
O2—V1—O1	74.67(8)	O2—V2—O1	79.87(9)
O3—V1—O1	173.24(13)	O4—V2—O1	101.32(11)
O6—V1—O1	84.23(10)	O1—V2—O5	81.03(9)
O6—V1—O2	91.00(10)	O2—V2—O5	82.46(9)
O3—V1—O2	101.77(13)	O4—V2—O2	100.24(11)
O3—V1—O6	101.76(14)	O4—V2—O5	176.66(11)
N1—V1—O1	78.21(9)	O1—V2—N3	106.07(10)
O2—V1—N1	95.27(10)	O2—V2—N3	162.20(11)
O3—V1—N1	96.58(12)	O4—V2—N3	95.06(12)
O6—V1—N1	158.44(12)	O1—V2—N4	161.15(10)
O2—V1—N2	160.64(10)	O2—V2—N4	91.59(10)
O3—V1—N2	97.35(13)	O4—V2—N4	96.71(12)
O6—V1—N2	87.03(11)	N3—V2—O5	81.97(9)
N2—V1—N1	79.43(11)	N4—V2—O5	81.19(10)
N2—V1—O1	86.00(10)	N3—V2—N4	77.53(11)

Many dinuclear vanadium(IV) complexes have been reported in the literature. For all complexes, the ligands are coordinated in *facial* or *meridional* conformation [36, 37]. In particular, complexes containing NNO-tridentated and sulfate ligands brigde-coordinated to oxovanadium(IV) such as $[(L^{1-})_2(V^{IV}O)_2(SO_4)]\cdot\frac{1}{2}CH_2Cl_2(6\cdot\frac{1}{2}CH_2Cl_2)$, where L is (E)-2-((quinolin-8-ylimino)methyl)phenol were described [36]. In this complex both tridentated L ligands adopt the *mer* conformation in contrast to observed in the complex described in this work. A dinuclear oxovanadium(VI) complex, $[\{VO(sal\text{-}aembz)\}_2SO_4].2H_2O$, where sal-aembz was obtained from the reaction between from salicylaldehyde and 2-aminoethylbenzimidazol, also contains one sulfate and two phenoxide moieties of the *mer*-sal-aembz bridge-coordinated to the

metal [36] having the V=O bonds oriented anti-coplanar, different than observed for $[(VO)_2(\mu\text{-HBPA})_2(\mu\text{-}SO_4)].4.75H_2O$.

Short contacts between the non-coordinated oxygen atoms of sulfate group and two oxygen atoms of lattice water molecules are observed with distances O7···O10 and O8···O9 of 2.791(8) and 2.698(7) Å, respectively for $[(VO)_2(\mu\text{-HBPA})_2(\mu\text{-}SO_4)].4.75H_2O$. Other intermolecular short contacts were also observed between the lattice water molecules. These water molecules are located in the space between $[(VO)_2(\mu\text{-HBPA})_2(\mu\text{-}SO_4)]$ molecules, mainly along the 1D channels parallel to the crystallographic *c* axis (Fig.2). These intermolecular interactions contribute to stabilize the crystal packing of the complex.

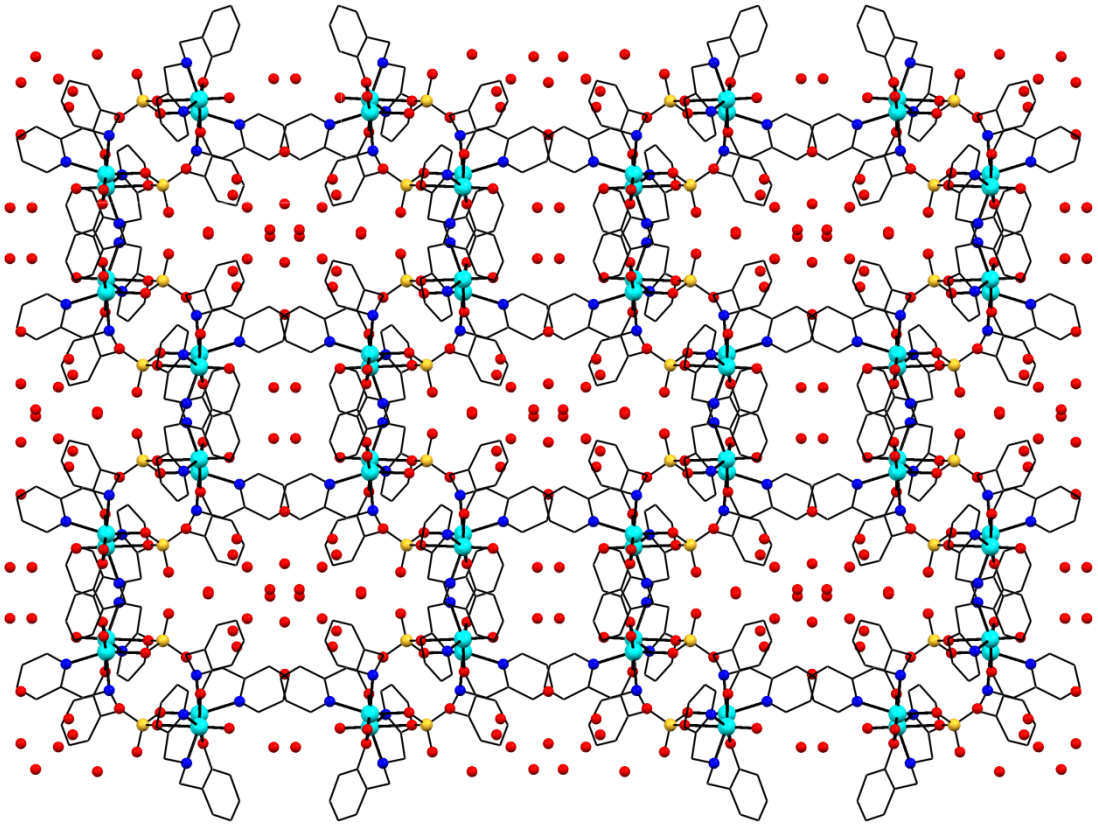

Fig. 2. View of the crystal packing of $[(VO)_2(\mu\text{-HBPA})_2(\mu\text{-}SO_4)].4.75H_2O$ along the crystallographic *c* axis. Hydrogen atoms were omitted for the sake of clarity.

3.2. Density functional theory (DFT) studies

The structure of the complex was optimized in a triplet state by means of the DFT/B3LYP method along the LAN2DZ basis set (Fig. 3). The absence of negative normal modes in frequency calculations emphasizes that the optimized structures are in minimum energies. The optimized structure is similar to the structure obtained by X-ray diffraction, the bonding lengths of the metal centers differ by a maximum of 5% and the angles by 7%, which indicates that the methodology used for the calculations was efficient. The computed values of the electronic chemical potential (μ) and global hardness are -0.14463 eV and (η) of 0.06766 eV, respectively. The global hardness (η) measures the stability of a system in terms of resistance to electron transfer and the chemical potential (μ) characterizes the escaping tendency of electrons from the equilibrium system [38]. The dipole moment calculated for the optimized structure is 12.6800 D, indicating a high polarity.

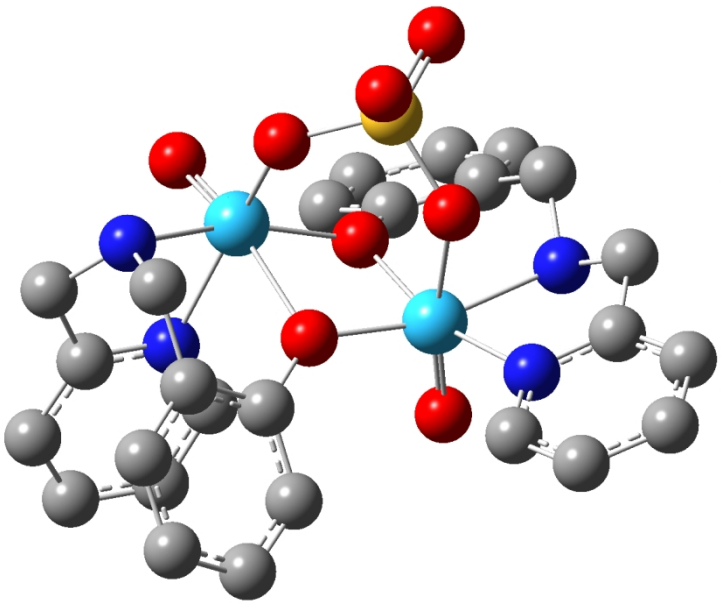

Fig. 3. Structure optimized by DFT using B3LYP functional and LANL2DZ basis set without hydrogen atoms. Colors: gray for C, red for O, cyan for V, yellow for S and blue for N.

Frontier molecular orbitals have an effective role for providing an insight into the chemical activities and some of the physical properties of the molecule [39]. The frontier molecular orbitals of the complex are shown in Fig. 4. Singly Occupied Molecular Orbital (SOMO) of α-spin in the complex have 21% V

character, 16% sulfate character along with 60% of ligand orbitals contribution (phenol, amine and pyridine donors). Similarly, LUMO of α-spin have 22% V character, 14% sulfate character along with 57% of ligand orbitals contribution. In both SOMO and LUMO formation, it was observed a similar and smaller contribution of oxo orbitals, about 3% and 7%, respectively.

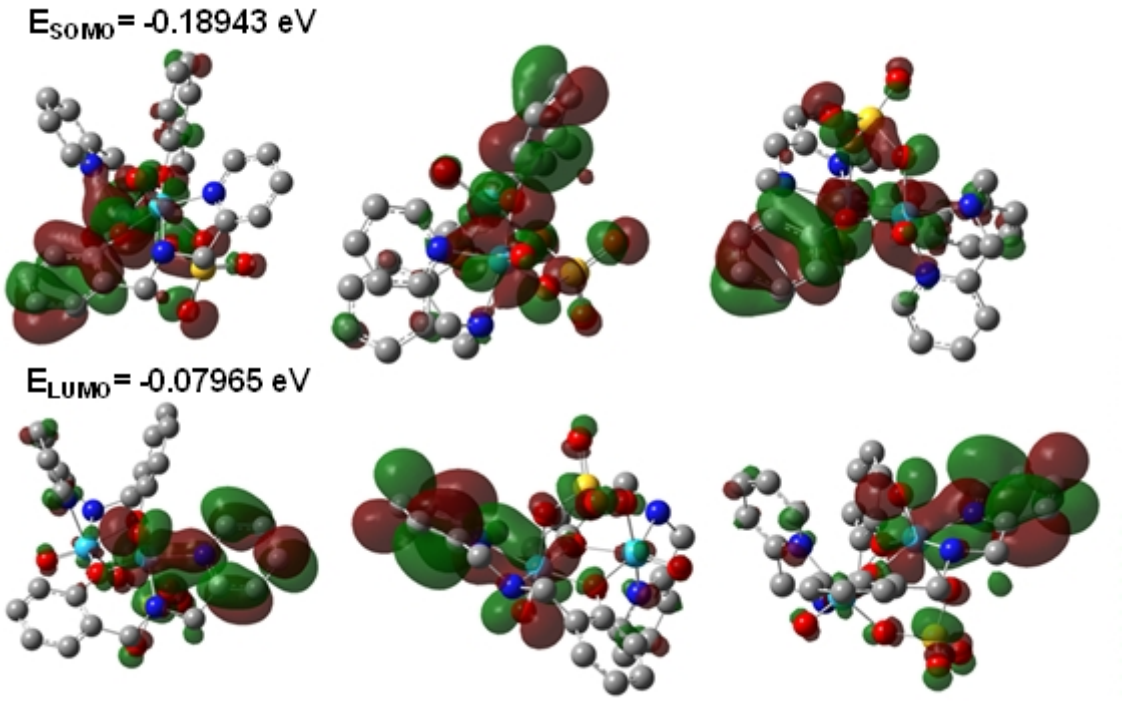

Fig. 4. Frontier molecular orbitals of $[(VO)_2(\mu\text{-HBPA})_2(\mu\text{-}SO_4)]$**:** SOMO (top) and LUMO (bottom).

The calculated Mulliken charges for complex are shown in Table 3. The Mulliken charge of vanadium atom is considerably lower than the formal charge of 4+ which confirms a significant charge donation from the ligands to the metal core. Furthermore, the Mulliken charge on the terminal oxygen atom (oxo group) is significantly less negative than 2-. Also, the Mulliken charge on oxygen atoms from the ligand are significantly less negative than 1- which can be attributed to electron density delocalization from these oxygen atoms towards the vanadium centers. The terminal oxygen atoms from oxo group are less negative in comparison with the oxygen atoms from the ligand which is related to higher electron density delocalization from the terminal oxo towards

the vanadium centers and agrees with the observed differences in bond lengths between each vanadium center and the oxygens from phenol groups (O1 and O2) and from oxo groups (O3 and O4), shown in Table 2.

Table 3. Selected calculated atomic Mulliken charges for $[(VO)_2(\mu\text{-HBPA})_2(\mu\text{-}SO_4)]$.

Atom	Mulliken charges
V1	+0.979
V2	+0.814
O1(phenol)	-0.638
O2(phenol)	-0.702
N2	-0.476
N4	-0.465
O5(sulfate)	-0.685
O6(sulfate)	-0.671
O3(oxo)	-0.362
O4(oxo)	-0.398

3.3. Characterization

3.3.1. Infrared vibrational spectroscopy (FTIR)

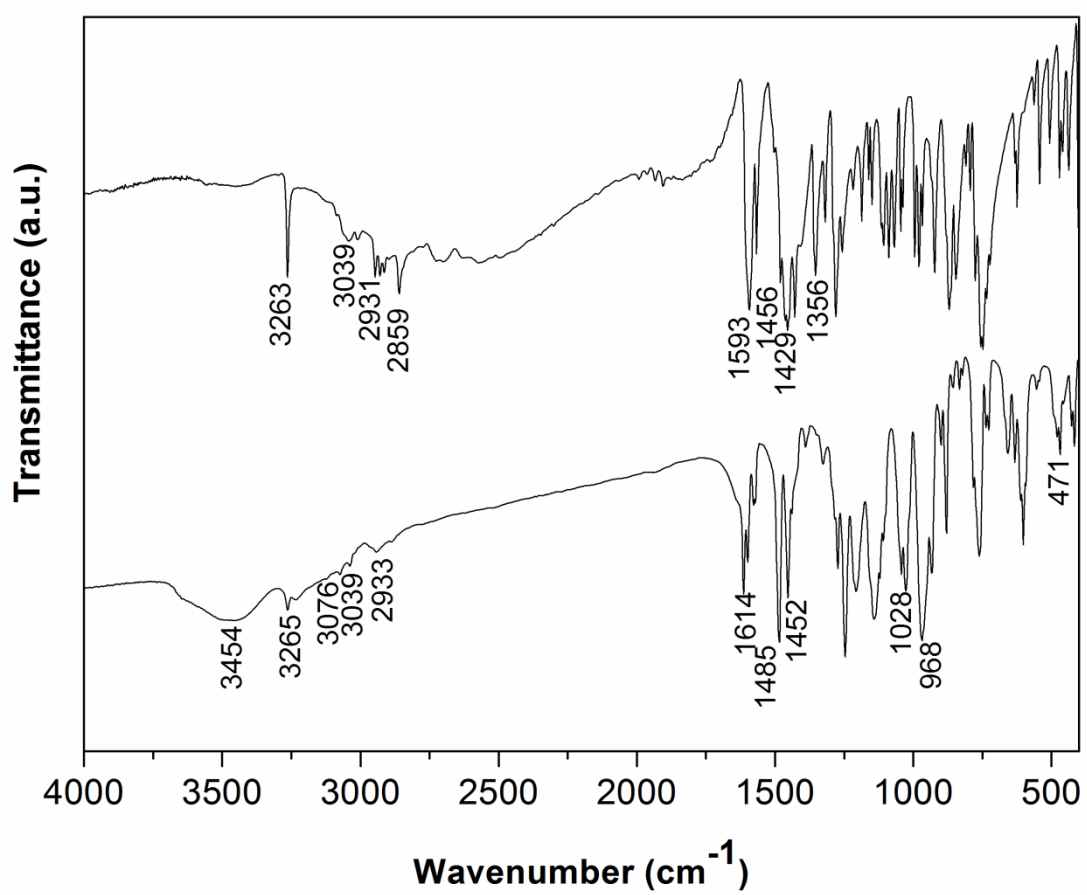

Fig. 5. FTIR spectra for HPBA ligand (top) and $[(VO)_2(\mu\text{-HBPA})_2(\mu\text{-}SO_4)].4.75H_2O$ (bottom).

The spectrum of HBPA (Fig. 5) shows a sharp band at 3263 cm^{-1} is attributed to N-H bond stretching from secondary amine. The weak band observed in 3039 cm^{-1} was attributed to aromatic νC-H while symmetric and asymmetric stretching of C-H bonds from methylene group are attributed to the bands at 2931 cm^{-1} and 2859 cm^{-1}, respectively. The bands at 1593, 1456 and 1429 cm^{-1} corresponds to the νC=N and νC=C from pyridine and phenol of the ligand. The band at 1356 cm^{-1} is related to the angular deformation of O-H bond from phenol group [35].

The IR spectrum of $[(VO)_2(\mu\text{-HBPA})_2(\mu\text{-}SO_4)].4.75H_2O$ (Fig. 5) shows a broad band at 3454 cm^{-1} that refers to the stretching of O-H bonds attributed to lattice water molecules involved in hydrogen bondings. As observed for the HBPA, the sharp band in 3265 cm^{-1} is attributed to νN-H bond indicating that the amine was not deprotonated after the coordination of the ligand to

vanadium(IV) ions. The aromatic νC-H was assigned to the bands at 3076, 3039 cm^{-1} and the aliphatic νC-H of methylene group were observed at 2933 cm^{-1} (symmetric) and 2860 cm^{-1} (asymmetric). The bands attributed to νC=N or νC=C at 1614, 1485, 1452 cm^{-1} were shifted to higher wavenumbers when compared to the ligand itself, indicating the coordination through the donor atoms of pyridine and phenoxide moieties of the ligand to the vanadium ion. An evidence of phenoxide formation is the disappearance of the band related to δO-H. The vanadyl (V=O) stretching is observed at 968 cm^{-1}, suggesting the presence of vanadium(IV) ions. The V-O stretching is assigned to the band at 405 cm^{-1} while the νV-N can be attributed to the band at 471 cm^{-1} [40, 41]. The IR data are summarized in Table 4.

Table 4. Mainly absorptions (cm^{-1}) attributed to the stretching in the vibration spectra of the HBPA ligand and $[(VO)_2(\mu\text{-HBPA})_2(\mu\text{-}SO_4)].5.5H_2O$.

HBPA	Complex	Group vibration
-	3454	νO-H (water)
3263	3265	νN-H (secondary amine)
3039	3076, 3039	νC-H (aromatic)
2931	2933	νC-H (aliphatic, symmetrical)
2859	2860	νC-H (aliphatic, unsymmetrical)
1593, 1456, 1429	1614, 1485, 1452	νC=C, νC=N (double bonds in aromatics)
1356	-	δO-H (phenol)
-	1028	νS=O (sulfate ion)
-	968	νV=O (vanadyl)
-	471	νN-V

3.3.2. Ultraviolet visible electronic spectroscopy

The electronic spectrum of $[(VO)_2(\mu\text{-HBPA})_2(\mu\text{-}SO_4)].4.75H_2O$ dissolved in methanol (Fig. 6) shows strong bands at 208 nm, 260 nm, and a shoulder at

282 nm, attributed to a intraligand transitions π-π*, as usually observed in aromatic compounds, such as phenol and pyridine rings. At 383 nm, it is observed a weak broad band that may be assigned to the phenoxide to vanadium charge transfer (LMCT p-π orbital), and the two bands (550 nm and 769 nm) observed at lower energy are attributed to the d-d transitions of vanadium ions [40, 21].

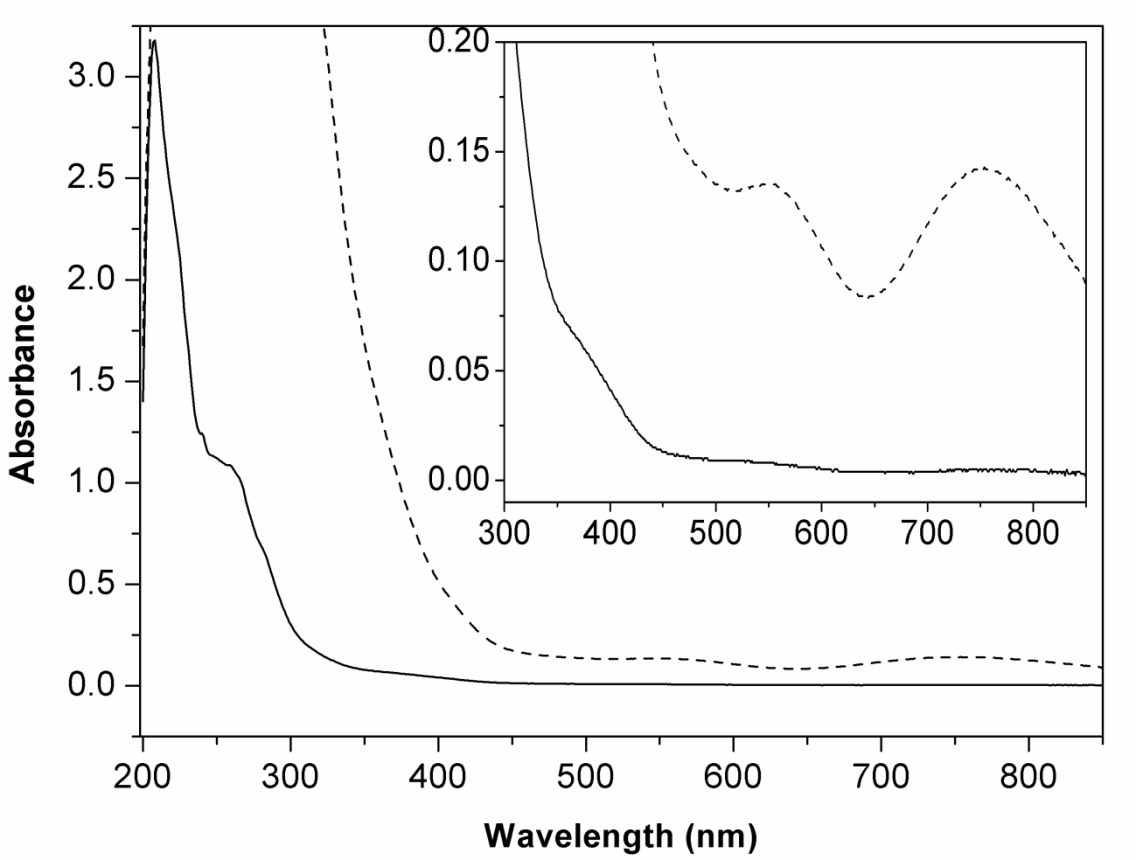

Fig. 6. Electronic spectra of complex $[(VO)_2(\mu\text{-HBPA})_2(\mu\text{-SO}_4)].4.75H_2O$ at $1.75x10^{-4}$ mol L^{-1} (straight line) and $7.00x10^{-3}$ mol L^{-1} (dashed line). Inset: zoom.

3.3.3. [ESI-(+)-MS]

ESI-(+)-MS spectrum of complex $[(VO)_2(\mu\text{-HBPA})_2(\mu\text{-SO}_4)].4.75H_2O$ (Fig. 7) was obtained in methanol and showed the presence of eight peaks. The most stable fragment corresponded the protonated HBPA, $[C_{13}H_{15}N_2O]^+$, at m/z 215.1. The peak at m/z 298.1 is the mononuclear complex $[(VO)(OH)(HBPA)]^+$. The peak at m/z = 608.1 corresponds to a fragment composed by a mononuclear vanadium(IV) complex containing two units of HBPA ligand and

one sulfate ion, $[(VO)(HBPA)_2(SO_4)]^+$. The most important fragment observed, m/z = 657.0, is a dinuclear oxovanadium(IV) with two units of the HBPA ligands, connected by a sulfate bridge, corresponding to the complex $[(VO)_2(HBPA)_2(\mu\text{-}SO_4)]^+$ as observed in the structure solved by single crystal X ray study. Fragments with higher mass can be probably formed in the gaseous phase as clusters obtained by reaction between fragments with lower mass, as we propose for the peak at m/z = 871 and 936.1. The first one corresponds to a dinuclear species containing a fragment of m/z 657 plus one unit of HBPA ligand. The second one, at m/z 936, is possibly formed for three species of mononuclear oxovanadium(IV), with structure $[(VO)(HBPA)]^+$ added to one sulfate ion.

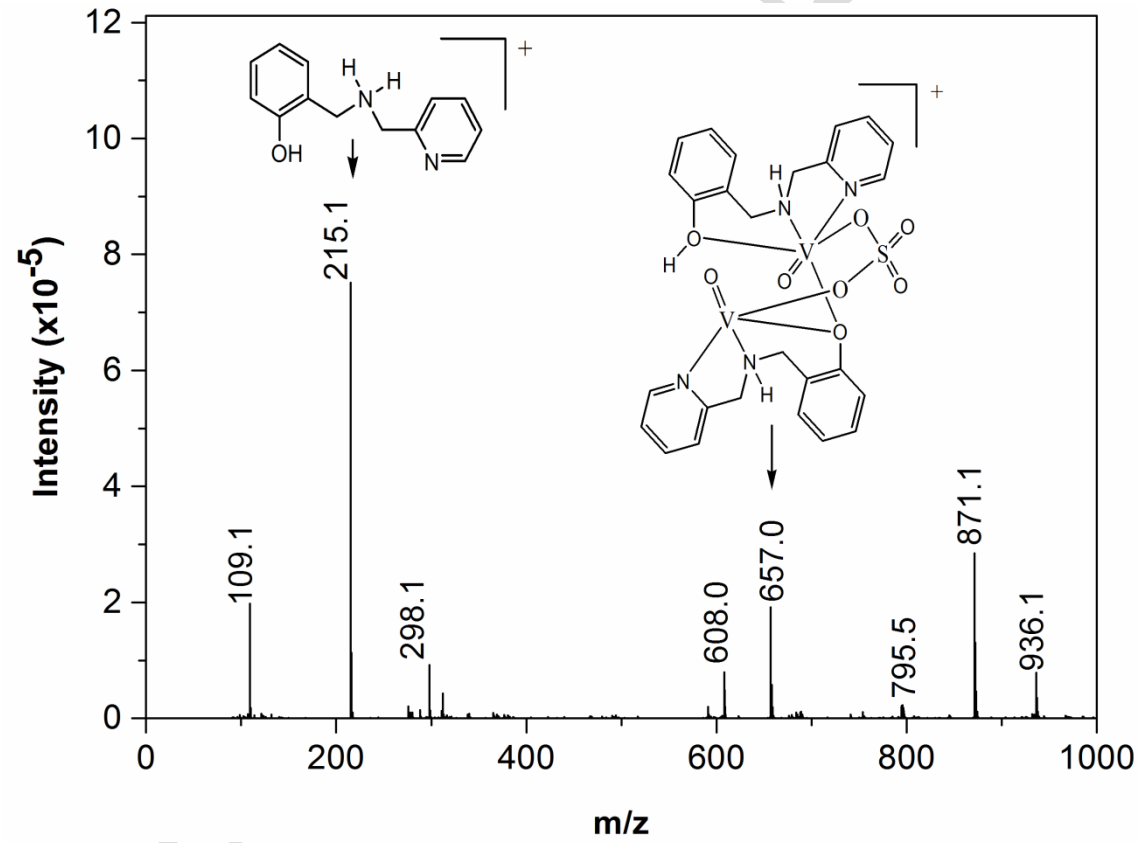

Fig. 7. Mass spectrum of $[(VO)_2(\mu\text{-}HBPA)_2(\mu\text{-}SO_4)].4.75H_2O$ in methanol solution.

3.3.4. Thermogravimetric analysis

Thermogravimetric analysis (TGA) was used to investigate the thermal stability of the complex. The TGA curve shows two defined weight losses (Fig.8). The first one is attributed to the loss of 8.8% of mass that is associated to the loss of 3.75 lattice water molecules (calc. 9.1%) in temperatures smaller than 72 ºC. It is in agreement with other compounds reported in the literature that shows loss water lattice molecules usually below 100ºC [42]. A smooth loss of 1.8% of mass occurs in the temperature range 72-290ºC that can be attributed to the loss of one more water molecule (calc 2.4%). A second loss of mass started after 290ºC, and the total weight loss of 79.7% is observed up to 990ºC leading probably to vanadium(IV) dioxide (calc. 77.8%) [43].

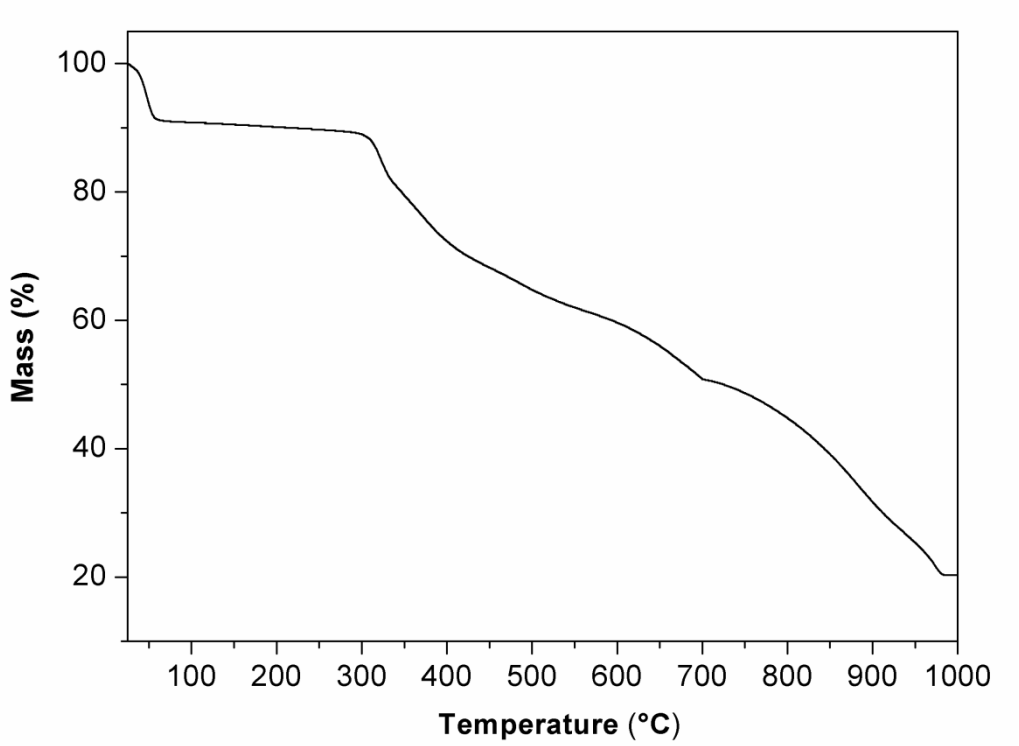

Fig. 2. TGA curve for $[(VO)_2(\mu\text{-}HBPA)_2(\mu\text{-}SO_4)].4.75H_2O$. The straight line represents the mass in percentage.

3.3.5. Electrochemical studies

The redox behavior of $[(VO)_2(\mu\text{-}HBPA)_2(\mu\text{-}SO_4)].4.75H_2O$ was investigated by cyclic voltametry. The cyclic voltammogram obtained in

methanol solution shows two irreversible electrochemical processes at anodic region (Fig. 9), the first one at +0.73 V and second one at +0.99V. This electrochemical behavior is common in dinuclear vanadium(IV) complexes at the anodic region [44] and it is attributed to the oxidation of both vanadium (IV) centers in two steps. The first one electron oxidation of one vanadium(IV) center from $V^{IV}V^{IV}$ to form the mixed valence complex $V^{V}V^{IV}$, followed by a second electron oxidation of vanadium(IV) center, producing the dinuclear pair $V^{V}V^{V}$ [45]. The variation of the potential scan rate in the electrochemical experiment produced the linear increasing of the peaks related to the oxidation processes (Fig. 9), which supports that the electron oxidation processes in both vanadium (IV) centers are controlled by diffusion mass transport in solution [46]. Then, it is observed a reduction at 0.11 V, which can be assigning as a partial reduction of the vanadium(V) pairs after oxidation.

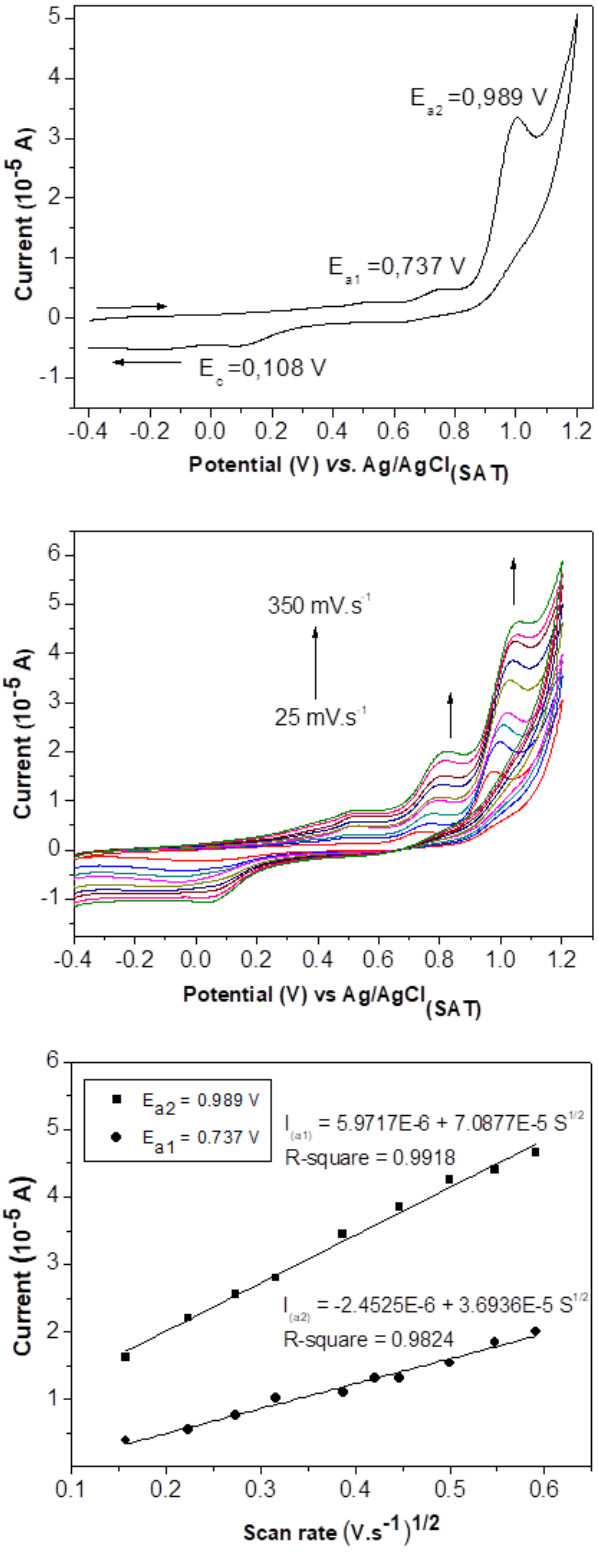

Fig. 3. Cyclic Voltammogram for $[(VO)_2(\mu\text{-HBPA})_2(\mu\text{-}SO_4)].4.75H_2O$ at 100 mV/s scan rate (top), cyclic voltammograms at scan rates of 25, 50, 75, 100, 150, 200, 250, 300 and 350 $mV.s^{-1}$ (middle) and linearity between current and scan rate ($S^{1/2}$) (bottom).

4. Conclusions

A new dinuclear vanadium(IV) complex $[(VO)_2(\mu\text{-HBPA})_2(\mu\text{-}SO_4)].4.75H_2O$ was synthesized. The structure was determined by single crystal X-ray diffraction, and the two vanadium ions are bridge coordinated moiety of HBPA ligand and sulfate ion. Although these two ions are coordinated by the same donor atoms, these ions have a quite different coordination environment being V1 and V2 coordinated by *fac*-HBPA and *mer*-HBPA conformations, respectively. This kind of coordination, having both *fac*- and *mer*- coordination environment is new for dinuclear vanadium(IV) complexes. The DFT studies for the complex, in agreement with the crystal structure, showed a high polarity. The stability can be confirmed by thermogravimetric analysis, where the crystal starts to degrade at temperature up to 300 °C, referred to the ligand loss. Electrochemical analysis was important to observe two irreversible electrochemical processes related to the oxidation of each vanadium(IV) ions.

Acknowledgements

We are thankful to LABEE (Universidade Federal do Rio de Janeiro) for support in electrochemical analysis, LCQUI (Universidade Estadual do Norte Fluminense) for ESI-MS analysis and LDRX-UFF (Universidade Federal Fluminense) for using its crystallographic facilities. RAAC acknowledges CNPq-Universal for financial support.

Supplementary Material

X-ray crystallographic data for $[(VO)_2(\mu\text{-HBPA})_2(\mu\text{-}SO_4)].4.75H_2O$ has been deposited as a CIF file at the Cambridge Crystallographic Data Center (CCDC code 1884251). This file can be obtained freely at http://www.ccdc.cam.ac.uk/structures.

References

[1] J. C. Pessoa, Thirty years through vanadium chemistry. *J. Inorg. Biochem.* 147, 2015, pp. 4-24. http://dx.doi.org/10.1016/j.jinorgbio.2015.03.004

[2] I. S. Fomenko, A. L. Gushchin, L. S. Shul'pina, N. S. Ikonnikov, P. A. Abramov, N. F. Romashev, A. S. Poryvaev, A. M. Sheveleva, A. S. Bogomyakov, N. Y. Shmelev, M. V. Fedin, G. B. Shul'pin, M. N. Sokolov. New oxodiovanadium(IV) complex with a BIAN ligand: synthesis, structure, redox properties and catalytic activity. *New J. Chem.* 42, 2018, pp. 16200-16210. https://doi.org/10.1039/C8NJ03358G.

[3] G. Licini, V. Conte, A. Coletti, M. Mba, C. Zonta. Recent advances in vanadium catalyzed oxygen transfer reactions. *Coord. Chem. Rev.* 255, 2011, pp. 2345-2357. https://doi.org/10.1016/j.ccr.2011.05.004

[4] A. Coletti, P. Galloni, A. Sartorel, V. Conte, B. Floris. Salophen and salen oxo vanadium complexes as catalysts of sulfides oxidation with H2O2: Mechanistic insights. *Catal. Today.* 192, 2012, pp. 44-55. http://dx.doi.org/10.1016/j.cattod.2012.03.032

[5] S. I. Pillai, S. P. Subramanian, M. Kandaswamy. A novel insulin mimetic vanadium–flavonol complex: Synthesis, characterization and in vivo evaluation in STZ-induced rats. *Eur. J. Med. Chem.* 63, 2013, pp. 109-117. http://dx.doi.org/10.1016/j.ejmech.2013.02.002

[6] T. Jakuscha, T. Kiss. In vitro study of the antidiabetic behavior of vanadium compounds. *Coord. Chem. Rev.* 351, 2017, pp. 118–126. http://dx.doi.org/10.1016/j.ccr.2017.04.007 0010-8545

[7] C. Rozzo, D. Sanna, E. Garribba, M. Serra, A. Cantara, G. Palmieri, M. Pisano. Antitumoral effect of vanadium compounds in malignant melanoma cell lines. *J. Inorg. Biochem.* 174, 2017, pp. 14-24. http://dx.doi.org/10.1016/j.jinorgbio.2017.05.010

[8] E. Kioseoglou,S. Petanidis, C. Gabriel, A. Salifoglou. The chemistry and biology of vanadium compounds in cancer therapeutics. *Coord. Chem. Rev.* 2015, Vols. 301–302, pp. 87–105. https://doi.org/10.1016/j.ccr.2015.03.010

[9] C. Datta, D. Das, P. Mondal, B. Chakraborty, M. Sengupta, C. R. Bhattacharje. Novel water soluble neutral vanadium(IV)–antibiotic complex:

Antioxidant, immunomodulatory and molecular docking studies. *Eur. J. Med. Chem.* 97, 2015, pp. 214-224. http://dx.doi.org/10.1016/j.ejmech.2015.05.005

[10] Z. H. Chohan, S. H. Sumrra, M. H. Youssoufi, T. B. Hadda. Metal based biologically active compounds: Design, synthesis, and antibacterial/antifungal/cytotoxic properties of triazole-derived Schiff bases and their oxovanadium(IV) complexes. *Eur. J. Med. Chem.* 45, 2010, pp. 2739-2747. http://dx.doi.org/10.1016/j.ejmech.2010.02.053

[11] M. S. S. Adam, H.Elsawy. Biological potential of oxo-vanadium salicylediene amino-acid complexes as cytotoxic, antimicrobial, antioxidant and DNA interaction. *J. Photochem. Photobiol., B* 184, 2018, pp. 34-43. https://doi.org/10.1016/j.jphotobiol.2018.05.002

[12] D. Gambino, Potentiality of vanadium compounds as anti-parasitic agents. *Coord. Chem. Rev.* 255, 2011, pp. 2193–2203. https://doi.org/10.1016/j.ccr.2010.12.028

[13] J. Benítez, A. C. de Queiroz, I. Correia, M. A. Alves, M. S. Alexandre-Moreira, E. J. Barreiro, L. M. Lima, J. Varela, M. González, H. Cerecetto, V. Moreno, J. C. Pessoa, D.Gambino. New oxidovanadium(IV) N-acylhydrazone complexes: Promising antileishmanial and antitrypanosomal agents. *Eur. J. Med. Chem.* 62, 2013, pp. 20-27. http://dx.doi.org/10.1016/j.ejmech.2012.12.036

[14] D. C. Crans, J. J. Smee, E. Gaidamauskas, L. Yang. The Chemistry and Biochemistry of Vanadium and the Biological Activities Exerted by Vanadium Compounds. *Chem. Rev.* 104, 2, 2004, pp. 849-902. http://dx.doi.org/10.1021/cr020607t

[15] K. Kikushima, T. Moriuchi, T. Hirao. Oxidative bromination reaction using vanadium catalyst and aluminum. *Tetrahedron Lett.* 51, 2010, pp. 340-342. https://dx.doi.org/10.1016/j.tetlet.2009.11.016

[16] F. Mendoza, R. Ruíz-Guerrero, C. Hernández-Fuentes, P. Molina, M. Norzagaray-Campos, E. Reguera. On the bromination of aromatics, alkenes and alkynes using alkylammonium bromide: Towards the mimic of bromoperoxidases reactivity. *Tetrahedron Lett.* 57, 2016, pp. 5644-5648. http://doi.org/10.1016/j.tetlet.2016.11.011

[17] B. Floris, F. Sabuzi, A. Coletti, V. Conte. Sustaintable vanadium-calayzed oxidation of organic substrates with H2O2. *Catal. Today* 285, 2017, pp. 49-56. http://dx.doi.org/10.1016/j.cattod.2016.11.006

[18] S. Menati, H. A. Rudbari, M. Khorshidifard, F. Jalilian. A new oxovanadium (IV) complex containing an O,N-bidentate Schiff base ligand: Synthesis at ambiente temperature, chacacterization, crystal structure and catalytic performance in selective oxidation of sulfides to sulfones using H2O2 under solvent free conditions. *J. Mol. Struct.* 1103, 2016, pp. 94-102. https://doi.org/10.1016/j.molstruc.2015.08.060

[19] M. R. Maurya, M. Bisht, F. Avecilla. Synthesis, characterization and catalytic activities of vanadium complexes containing ONN donor ligand derived from 2-aminoethylpyridine. *J. Mol. Catal. A: Chem.* 344, 2011, pp. 18-27. https://doi.org/10.1016/j.molcata.2011.04.017

[20] G. Romanowski, J. Kira, M. Wera. Five- and six-coordinate vanadium(V) complexes with tridentate Schiff base ligands derived from *S*(+)-isoleucinol: Synthesis, characterization and catalytic activity in the oxidation of sulfides and olefins. *Polyhedron* 67, 2014, 529-539. https://doi.org/10.1016/j.poly.2013.10.008

[21] J. Pisk, J. C. Daran, R. Poli, D. Agustin. Pyridoxal based ONS and ONO vanadium(V) complexes: Structural analysis and catalytic application in organic solvent free epoxidation. *J. Mol. Catal. A: Chem.* 403, 2015, pp. 52-63. http://dx.doi.org/10.1016/j.molcata.2015.03.016

[22] C-J Yu, M. J. Graham, J. M. Zadrozny, J. Niklas, M. D. Krzyaniak, M. R.Wasielewski, O. G. Poluektov, D. E. Freedman. Long Coherence Times in Nuclear Spin-Free Vanadyl Qubits. *J. Am. Chem. Soc.* 138, 2016, pp. 14678-14685. https://doi.org/10.1021/jacs.6b08467

[23] M. Atzori, A. Chiesa, E. Morra, M. Chiesa, L. Sorace, S. Carretta, R. Sessoli. A two-qubit molecular architecture for electron-mediated nuclear quantum simulation. *Chem. Sci.* 9, 2018, pp. 6183-6192. https://doi.org/10.1039/c8sc01695j

[24] M. Atzori, E. Morra, L. Tesi, A. Albino, M. Chiesa, L. Sorace, R. Sessoli. Quantum Coherence Times Enhancement in Vanadium(IV)-based Potential

Molecular Qubits: the Key Role of the Vanadyl Moiety. *J. Am. Chem. Soc.* 138, 2016, pp. 11234-11244. https://doi.org/10.1021/jacs.6b05574

[25] S. Dekar, K. Ouari, S. Bendia, D. Hannachi, J. Weiss. Mononuclear oxovanadium(IV) Schiff base complex: Synthesis, spectroscopy, electrochemistry, DFT calculation and catalytic activity. *J. Organomet. Chem.* 866, 2018, pp. 154-176. https://doi.org/10.1016/j.jorganchem.2018.04.015

[26] P. Mahaboubi-Anarjan, R. Bikas, H. Hosseini-Monfared, P. Aleshkevych, P. Mayer. Synthesis, characterization, EPR spectroscopy and catalytic activity of a new oxidovanadium(IV) complex with N2O2-donor ligand. *J. Mol. Struct.* 1131, 2017, pp. 58-265. https://doi.org/10.1016/j.molstruc.2016.11.059

[27] N. Noshiranzadeh, M. Enami, R. Bikas, J. Sanchiz, M. Otrepa, P. Aleshkevych, T. Lis. Synthesis, characterization and magnetic properties of a dinuclear oxidovanadium(IV) complex: Magneto-structural DFT studies on the effects of ou-of-plane -OCH3 angle. *Polyhedron* 122, 2017, pp. 194-202. https://doi.org/10.1016/j.poly.2016.11.026

[28] Z. Chi, , L. Zhu, X. Lu. Comparison of two binuclear vanadium-cathecolate complexes: synthesis, X-ray structure and effects in cancer cells. *J. Mol. Struct.* 1001, 2011, pp. 111-117. https://doi.org/10.1016/j.molstruc.2011.06.026

[29] D. F. Back, G. M. Oliveira, L. A. Fontana, A. Neves, B. A. Iglesias, T. P. Camargo, P. T. Campos, J. P. Vargas. New dioxidodouranium (VI) and mixed valence oxidovanadium (IV/V) coordination compounds with N,O-pentadentate ligands obtained from pydodoxal and triethylenetetramine. *Inorganica Chimica Acta.* 2015, Vol. 428 , pp. 163–169. https://doi.org/10.1016/j.ica.2015.01.013

[30] Bruker. SAINT and APEX2. Bruker-Nonius AXS Inc. Madison, Wisconsin, USA, 2015.

[31] G. M. Sheldrick. *SADABS, Program for Empirical Absorption Correction of Area Detector Data.* Germany, University of Gottingen, 1996.

[32] G. M. Sheldrick. Crystal structure refinement with SHELXL. *Acta Cryst. C.,* 2015, pp. 3-8. https://doi.org/10.1107/S2053229614024218

[33] C. K. Johnson. An Introduction to Thermal Motion Analysis. F. R. Ahmed, Munksgaard, Copenhagen, Denmark, 1970. pp. 207-219.

[34] Gaussian 09, Revision A.1, M.J. Frisch, G.W. Trucks, H.B. Schlegel, G.E. Scuseria, M.A. Robb, J.R. Cheeseman, G. Scalmani, V. Barone, B. Mennucci,

G.A. Petersson, H. Nakatsuji, M. Caricato, X. Li, H.P. Hratchian, A.F. Izmaylov, J. Bloino, G. Zheng, J.L. Sonnenberg, M. Hada, M. Ehara, K. Toyota, R. Fukuda, J. Hasegawa, M. Ishida, T. Nakajima, Y. Honda, O. Kitao, H. Nakai, T. Vreven, J.A. Montgomery, Jr., J.E. Peralta, F. Ogliaro, M. Bearpark, J.J. Heyd, E. Brothers, K.N. Kudin, V.N. Staroverov, R. Kobayashi, J. Normand, K. Raghavachari, A. Rendell, J.C. Burant, S.S. Iyengar, J. Tomasi, M. Cossi, N. Rega, J.M. Millam, M. Klene, J.E. Knox, J.B. Cross, V. Bakken, C. Adamo, J. Jaramillo, R. Gomperts, R.E. Stratmann, O. Yazyev, A.J. Austin, R. Cammi, C. Pomelli, J.W. Ochterski, R.L. Martin, K. Morokuma, V.G. Zakrzewski, G.A. Voth, P. Salvador, J.J. Dannenberg, S. Dapprich, A.D. Daniels, Ö. Farkas, J.B. Foresman, J.V. Ortiz, J. Cioslowski, D.J. Fox, Gaussian Inc., Wallingford CT, 2009.

[35] A. Neves, C. N. Verani, M. A. de Brito, I. Vencato, A. Mangrich, G. Oliva, D. D. H. F. Souza, A. A. Batista. Copper(II) complexes with (2-hydroxybenzyl-2-pyridylmethyl)amine–Hbpa: syntheses, characterization and crystal structures of the ligand and [Cu(II)(Hbpa)2](ClO4)2·2H2O. *Inorg. Chim. Acta* 290, 1999, pp. 207-212. https://doi.org/10.1016/S0020-1693(99)00149-8

[36] M. Shit, S. Bera, S. Maity, T. Weyhermüller, P. Ghosh. Coordination of o-benzosemiquinonate, o-iminobenzosemiquinonate and aldimine anion radiocals to oxovanadium(IV). *New J. Chem.* 41, 2017, pp. 4564-4572. https://doi.org/10.1039/C7NJ00186J

[37] M. R. Maurya, A. Kumar, M. Ebel, D. Rehder. Synthesis, Characterization, Reactivity and Catalytic Potential of Model Vanadium(IV, V) Complexes with Benzimidazole-Derived ONN Donor Ligands. *Inorg. Chem.* 45, 2006, pp. 5924-5937. https://doi.org/10.1021/ic0604922

[38] S. Sengupta, A. Toro-Labbe. Estimating molecular electronic chemical potential and hardness from fragments' addition schemes. *J. Phys. Chem. A* 106, 17, 2002, pp. 4443-4444. https://doi.org/10.1021/jp020043x

[39] S. Xavier, S. Periandy, K. Carthigayan, S. Sebastian. Molecular docking, TG/DTA, molecular structure, harmonic vibrational frequencies, natural bond orbital and TD-DFT analysis of diphenyl carbonate by DFT approach. *J. Mol. Struct.* 1125, 2017, pp. 204-216. https://doi.org/10.1016/j.molstruc.2016.06.071

[40] M. R. Maurya, A. Arya, A. Kumar, M. L. Kuznetsov, F. Avecilla, J. C. Pessoa. Polymer-Bound Oxidovanadium(IV) and Dioxidovanadium(V) Complexes As Catalysts for the Oxidative Desulfurization of Model Fuel Diesel. *Inorg. Chem.* 49, 14, 2010, pp. 6586-6600. https://doi.org/10.1021/ic1004209

[41] A. HornJr., C. A. L. Filgueiras, J. L. Wardell, M. H. Herbst, N. V. Vugman, P. S. Santo, J. G. S. Lopes, R. A. Howie. A fresh look into VO(salen) chemistry: synthesis, spectroscopy, electrochemistry and crystal structrure of [VO(salen)(H2O)]Br.0,5 CH3CN. *Inorg. Chim. Acta* 357, 2004, pp. 4240-4246. https://doi.org/10.1016/j.ica.2004.06.023

[42] M. R. Maurya, S. Sikarwa. Oxidation of phenol and hidroquinone catalysed by copper(II) and oxovanadium(IV) complexes of N,N'-bis-(salicydelene)diethylenetriamine (H2saldien) covalently bonded to polystirene. *J. Mol. Catal. A: Chem.* 263, 2007, pp. 175-185. https://doi.org/10.1016/j.molcata.2006.08.038

[43] H. Barfeie, G. Grivani, V. Eigner, M. Dusek, A. D. Khalajic. Copper(II), nickel(II), zinc(II) and vanadium(IV) Schiff base complexes: synthesis, characterization, crystal structure determination, and thermal studies. *Polyhedron* 146, 2018, pp. 19–25. https://doi.org/10.1016/j.poly.2018.02.012

[44] L. Leelavathy, S. Anbu, M. Kandaswamy, N. Karthikeyan, N. Mohan. Synthesis and characterization of a new series of unsymmetrical macrocyclic binuclear vanadyl(IV) complexes: electrochemical, antimicrobial and DNA binding and clevage studies. *Polyhedron.* 2009, Vol. 28, pp. 903–910. https://doi.org/10.1016/j.poly.2008.12.062

[45] E. S. Bazhina, E. S. Bazhina, M. E. Nikiforova, G. G. Aleksandro, N. N. Efimov, H. A. Ugolkova, O. M. Nikitin, T. V. Magdesieva, A. S. Bogomyakov, V. V. Minin, A. A. Sidorov, V. M. Novotortsev, I. L. Eremenko. New sulfate-bridged dinuclear oxovanadium complexes. *Inorg. Chim. Acta.* 392, 2012, pp. 192–198. https://doi.org/10.1016/j.ica.2012.06.001

[46] C. Brett, A. M. O. Brett. Electroanalysis. Oxford Chemistry Primers. Oxford University Press, Oxford, 1998, pp 48-53.